

Supplementary information

Enhancing the photocatalytic activity of TiO₂ nanoparticles using green carbon quantum dots

1. Experimental details

1.1. Kinetic study of MB degradation

The study of the photocatalytic reaction kinetics of the MB was performed using initial MB concentrations of 5 mg/L, 7.5 mg/L, 10 mg/L, 12.5 mg/L, and 15 mg/L in a solution containing 250 mg of TiO₂ NPs. The kinetic order of MB degradation was assessed using Equations (S1) and (S2) [1]:

• Equation of pseudo-first-order kinetics:

$$\ln C_t - \ln C_0 = -k_1 t \quad (\text{S1})$$

• Equation of pseudo-second-order can be formulated as displayed by Equation (S2):

$$1/C_t - 1/C_0 = k_2 t \quad (\text{S2})$$

where C₀ and C_t are the initial and at different times t concentration of MB, respectively. The constants k₁ and k₂ are the velocity constants for pseudo-first-order and pseudo-second-order models, respectively.

The study of the adsorption isotherms of MB on TiO₂ NPs and TiO₂/CQDs was carried out for the following models:

• Langmuir-Hinshelwood model: The Langmuir-Hinshelwood model is widely used to describe experimental results in heterogeneous photocatalysis. This model is expressed by Equation (S1) rewritten as [1]:

$$\ln \left(\frac{C_0}{C_t} \right) = k_1 t \quad (\text{S3})$$

where C_t is the concentration of MB (mg/L) at irradiation time t, k₁ is the apparent degradation constant (min⁻¹) and t is the irradiation time (min).

• Temkin model: The Temkin isotherm takes into account the fact that the heat of adsorption of all the molecules in the overlying layer decreases linearly with the overlay due to the decrease in adsorbent-adsorbate interactions. Adsorption is characterized by a uniform distribution of binding energies at the surface. The Temkin isotherm is expressed according to Equation (S4) [2]:

$$q_e = (RT/b_t) \cdot \ln(K_t C_e) \quad (\text{S4})$$

30 or in the form of Equation (S5):

$$31 \quad q_e = B_1 \cdot \ln K_t + B_1 \cdot \ln C_e \quad (S5)$$

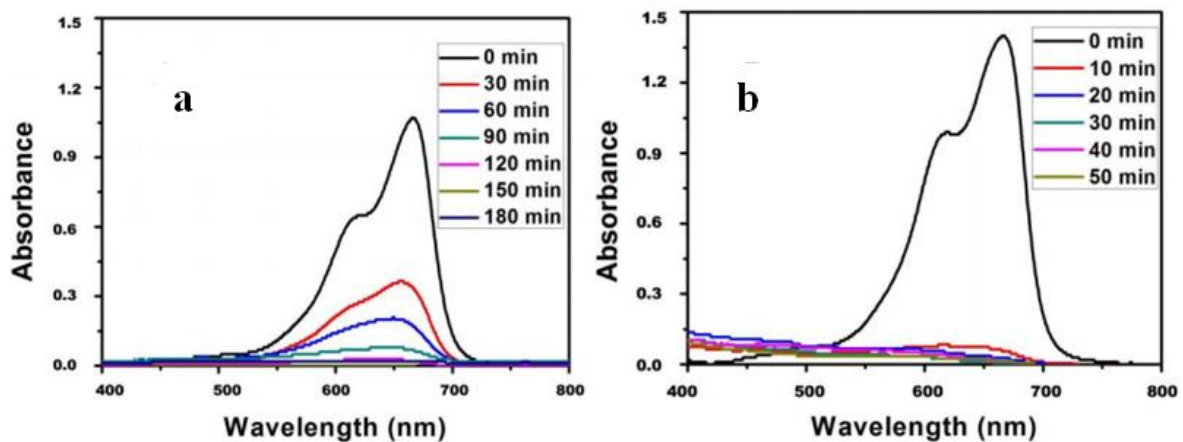
32 with B_1 is the Temkin's constant for the sorption characteristic, C_e the equilibrium concentration, and
33 K_t ($L \cdot g^{-1}$) the adsorption equilibrium constant corresponding to the maximum binding energy.

34 1.2. Application

35 In order to study the applicability of the synthesized TiO_2 NPs and $TiO_2/CQDs$ photocatalytic
36 properties in real samples, wastewater from the University Hospital Center of Cocody (UHCC) was
37 assessed after its contamination with MB. After sampling, the collected water was transferred to a 1 L
38 bottle, and quickly closed to avoid any air bubbles and the variation in CO_2 content, carbonate
39 precipitation and oxidation of the mineral elements. The bottle is placed in a cooler containing ice to
40 maintain the temperature at $4^\circ C$ until it reaches the laboratory. It should be mentioned that the
41 collected water is yellow in color with a temperature of $27.6^\circ C$, pH 8.4, conductivity of $836 \mu S/cm$
42 and water salinity of 1.7. As the electric current is carried by the ions in the solution, this high
43 conductivity suggests that this UHCC wastewater contains higher amount of ions.

44 2. Photocatalytic study of TiO_2 NPs and $TiO_2/CQDs$

45 All experiments were performed in the presence of 250 mg of TiO_2 NPs or $TiO_2/CQDs$ under sunlight
46 exposure at room temperature over time (**Figure S1**). In this figure, it can be observed that the
47 characteristic peak of MB around 664 nm disappears completely after certain times of irradiation,
48 suggesting that TiO_2 NPs and $TiO_2/CQDs$ are efficient photocatalysts for the complete degradation of
49 MB. This degradation is much more important in the case of $TiO_2/CQDs$. It should be noted that the
50 faster disappearance of MB using $TiO_2/CQDs$ compared to TiO_2 NPs is made possible by the addition
51 of CQDs which leads to the improvement of the photocatalytic properties of TiO_2 NPs.



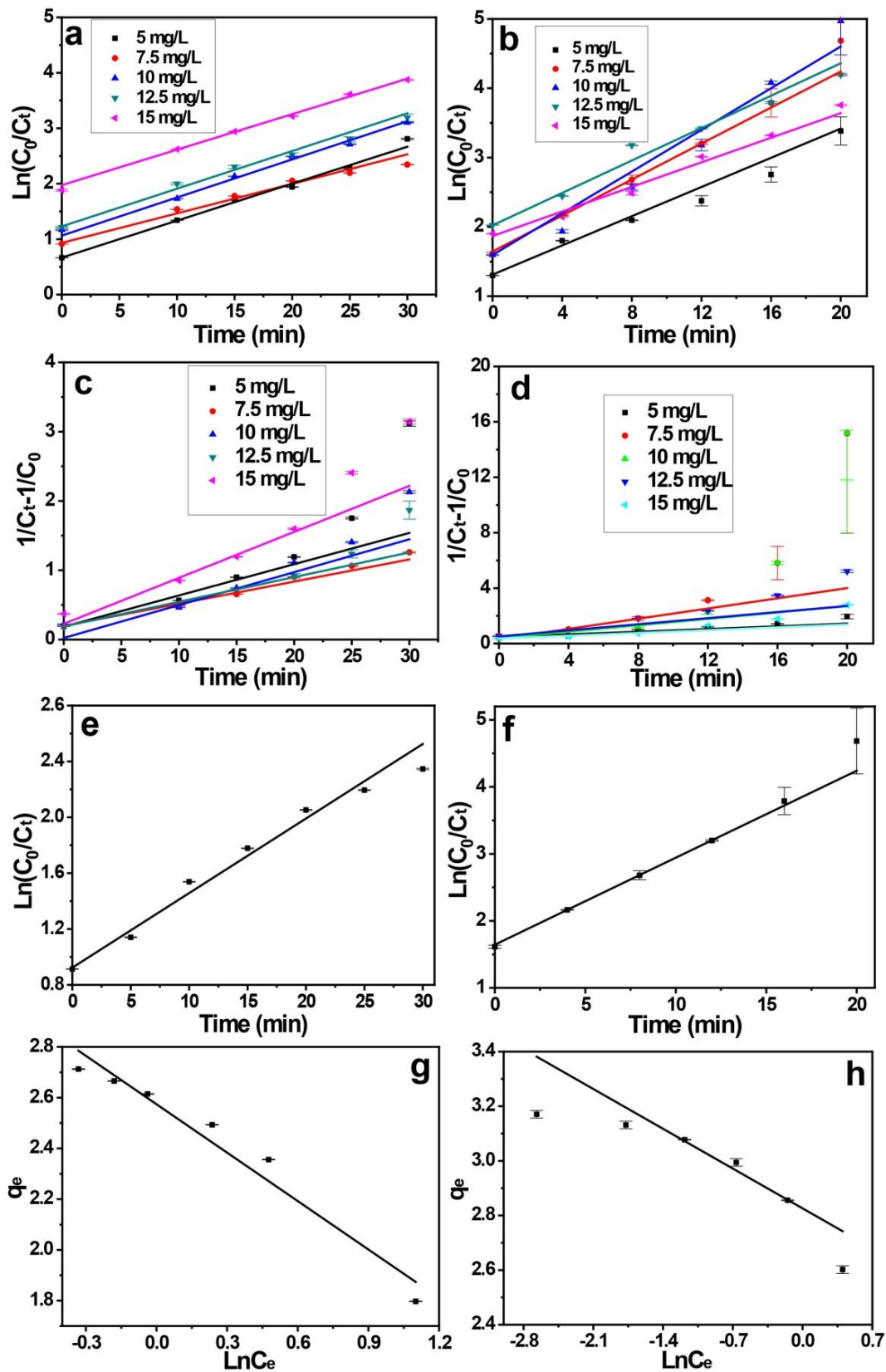
52

53

Figure S1: UV-Vis spectra of MB using a) TiO_2 NPs and b) $TiO_2/CQDs$ at different times

54

3. Kinetics of MB degradation



06

07 **Figure S2:** Degradation kinetics of pseudo-first order on a) TiO₂ NPs and b) TiO₂/CQDs, and pseudo-second order on c) TiO₂ NPs and d)
 08 TiO₂/CQDs, respectively. Langmuir-Hinshelwood kinetic model using 250 mg of e) TiO₂ NPs and f) TiO₂/CQDs, and Temkin kinetic model
 09 using 250 mg of g) TiO₂ NPs and h) TiO₂/CQDs of 7.5 mg/L MB, respectively

4. Calibration for the detection of residual MB after its degradation

In order to quantitatively study the relationship between the concentration of MB before and after the addition of TiO₂ NPs as a function of the irradiation time, the calibration curve is built by plotting the absorbance as a function of the different MB concentrations (0.25 mg/L, 0.5 mg/L, 1 mg/L, 1.5 mg/L, 2 mg/L, 2.5 mg/L, 3 mg/L, 3.5 mg/L, 4 mg/L, 4.5 mg/L, 5 mg/L, 7.5 mg/L, 10 mg/L, 12.5 mg/L and 15 mg/L) (**Figure S3**). The difference in absorbance (ΔA) between the maximum absorbance of MB before (A_0) and after the addition of TiO₂ NPs (A_i) was investigated to evaluate the residual MB. A linear range from 0.25 mg/L to 15 mg/L is obtained, leading to Equation (S6):

$$\Delta A = 0.032 \times C + 0.202 \quad (\text{S6})$$

with C in mg/L.

This equation is used to assess the MB residual concentration after degradation (0.36 mg/L is the calculated limit of detection).

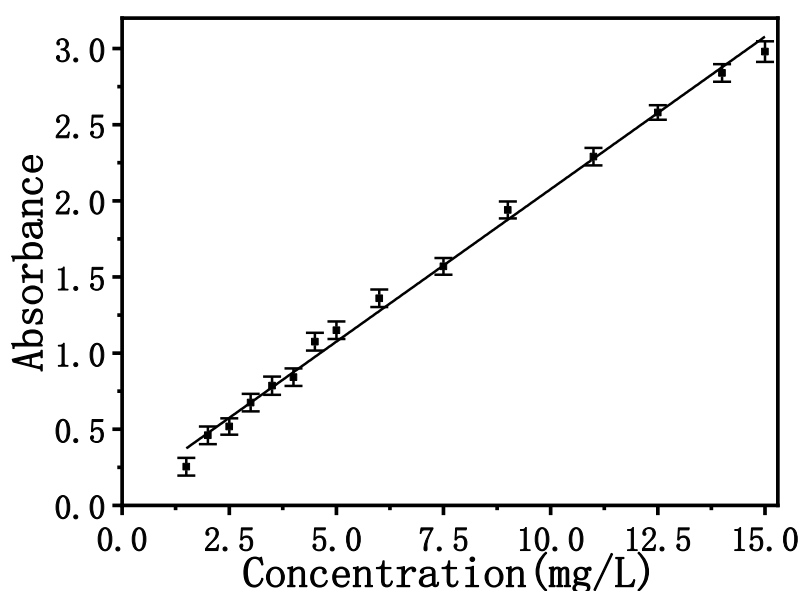
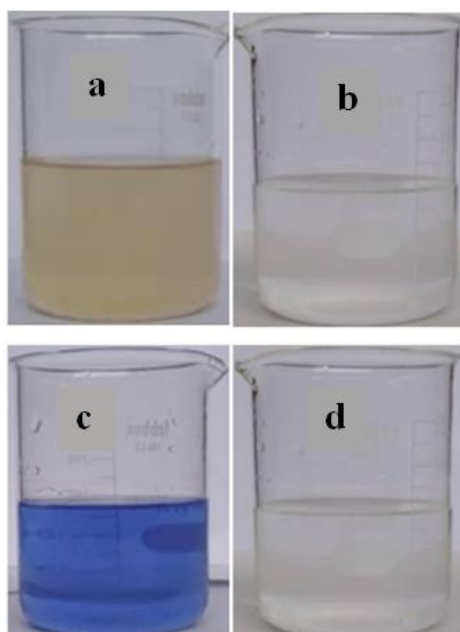


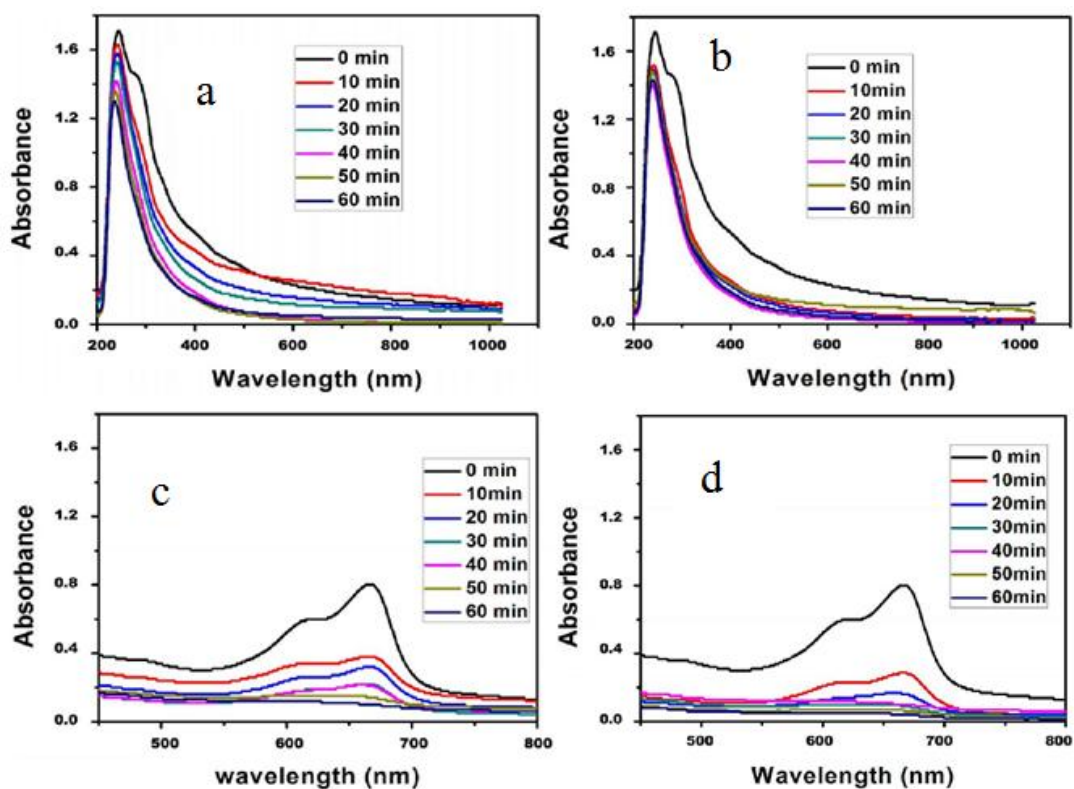
Figure S3: Calibration curve of MB for concentration ranging from 0.25 mg/L to 15 mg/L

5. Application of TiO₂ NPs and TiO₂/CQDs on the degradation of MB in UHCC wastewater

Figure S4 shows the pictures of the different solutions, the UHCC wastewater before and after sun exposure (**Figures S5a&b**) and the MB-contaminated UHCC wastewater before and after 50 min, and 30 min of sun exposure (**Figures S5c&d**) with TiO₂ NPs and TiO₂/CQD as photocatalyst, respectively. Importantly, the synthesized photocatalysts discolor the UHCC wastewater.



80
 81 **Figure S4:** UHCC wastewater a) before and b) after degradation and, the UHCC wastewater contaminated with 7.5 mg/L MB c) before and
 82 d) after degradation.



83
 84 **Figure S5:** UV-Vis spectra of UHCC wastewater using a) TiO_2 NPs and b) TiO_2/CQDs , and degradation on c) TiO_2 NPs and d) TiO_2/CQDs
 85 at different times of UHCC wastewater contaminated with BM. All experiments are done with exposure to sunlight.

86 **Figure S5** shows the UV-Vis spectra of UHCC wastewater (**Figure S5a** and **Figure S5b**) and UHCC
 87 wastewater contaminated with MB (**Figure S5c** and **Figure S5d**) using 250 mg of TiO_2 NPs or 250
 88 mg of TiO_2/CQDs under sun exposure at room temperature at different times. In **Figure S5a** and
 89 **Figure S5b**, the disappearance of the shoulder of the wastewater spectra during the irradiation time in

90 the presence of the photocatalysts (TiO₂ NPs and TiO₂/CQDs) is observed. Furthermore, in **Figure**
91 **S5c and Figure S5d**, it can be observed that the characteristic peak of MB around 664 nm disappears,
92 showing the degradation of MB in the contaminated UHCC wastewater by TiO₂/CQDs.

93

- 94 [1] Urbain, K. Y., Fodjo, E. K., Ardjouma, D., Serge, B. Y., Aimé, E. S., Marc, G. I., & Albert, T.,
95 (2017), Removal of imidacloprid using activated carbon produced from ricinodendron
96 heudelotii shells, *Bull. Chem. Soc. Ethiop.*, 31: 397-409.
- 97 [2] Kavitha, D., & Namasivayam, C., (2007), Experimental and kinetic studies on methylene blue
98 adsorption by coir pith carbon, *Bioresour. Technol.*, 98: 14-21.

99